

Scalar Measurements by Laser Induced Fluorescence

M.M.C.L. Lima^{(1)†}, J.M.L.M. Palma^{(2)‡} and P.M. Areal⁽³⁾

Faculdade de Engenharia da Universidade do Porto
Rua Dr. Roberto Frias s/n
4200-465 Porto, Portugal

⁽¹⁾ E-mail: mmlima@civil.uminho.pt
^(2, 3) E-mail: {jpalma, pareal}@fe.up.pt

ABSTRACT

This study is concerned with the measurements of scalar variables in turbulent flows, by Laser Induced Fluorescence. We used solutions of water and rhodamine B, to study the properties of the fluorescent tracer and the characteristics of the fluorescence signal and its dependence on the instrumentation and other experimental conditions.

It is shown that a linear relationship between light intensity and concentration is obtained, for laser power up to 600 mW and rhodamine B concentration up to 0.08 mg/l. We also demonstrated that the light absorption along the path was negligible for concentrations below 0.04 mg/l and defined the parameters for reliable measurements up to 2 mm away from the wall.

The experimental uncertainty, determined in accordance with recent recommendations, was found to be between 5.5 and 15.6%. Based on the bootstrap technique, the confidence intervals downgraded as the order of the statistical moments increased. Flatness could be measured with a maximum uncertainty of about 25%.

[†] Current address: Escola de Engenharia da Universidade do Minho, Campus de Azurém, 4800-058 Guimarães, Portugal

[‡] Corresponding author.

1. INTRODUCTION

The laser-induced fluorescence (LIF) is a non-intrusive, optical, technique for concentration measurements, well established in the analytical chemistry field (Guilbault, 1990), where it is called fluorescent spectroscopy. A fundamental approach to the LIF as a technique for study of scalar turbulent transport can be found in Walker (1987) and the first simultaneous measurements using LIF and laser Doppler velocimetry (LDV) is usually attributed to Owen (1976).

Only the simultaneous measurements of velocity and scalar quantities enable the evaluation of the turbulent transport, providing a deeper understanding of the turbulent mixing and assisting the development of mathematical models. Laser induced fluorescence may easily be added as an extension to LDV systems and this line of development has been pursued by some manufacturers, e.g. Dantec (2002). The LDV is a light frequency, whereas the laser induced fluorescence is a light intensity based experimental technique. This poses a series of new experimental difficulties that may require attention to aspects, ignored in other experimental techniques, such as LDV, hindering a wider use of LIF in fluid mechanics research.

LIF is an extremely high sensitivity experimental technique, and values of up to 10^{-10} M have been reported in amine and amino acid analysis (Nouadje et al., 1996); however, this advantage, can easily become a drawback, because requires great care in the preparation of the concentrated solutions of fluorescent tracer to be injected in test rigs as used in fluid mechanics laboratories. The fluorescent emission can be reduced, quenching, by a deactivation process, due to the interaction between the fluorescent compound and another substance, by ultraviolet light (Guilbault, 1990), temperature, oxygen or impurities in the solution. A high fluorescence signal is desirable, to enhance the signal to noise ratio and the system resolution. However, if the concentration is too high, light absorption may occur along the beam path (inner-cell effect in fluorescent spectroscopy applications, Guilbault, 1990) or compounds made out of several fluorescent molecules may be formed, resulting in lower quantum efficiency and alteration of the absorption and emission spectra of the fluorescent compound. Signal saturation may occur as consequence of high incident radiation in solutions that are not stirred, and the fluorescence intensity diminishes as the incident radiation increase (Walker, 1987). This may be avoided if the solution residence time inside the control volume is lower than the photodecomposition temporal constant (20 s for rhodamine 6G, see Koochesfahani, 1984) by continuously stirring the solutions. This also avoids thermal booming, i.e. the localized heating of solution due to the laser beam, that originates refraction index gradients, divergence of the incident laser beam and therefore lower fluorescence intensity. There are few analysis of the noise associated with light intensity measurements, being Wang and Fiedler (2000 a,b) a recent exception, however and despite a wider use of LIF, a thorough analysis of the influence of the experimental conditions is still missing when it comes to applications in fluid mechanics.

In summary, a plethora of physical and chemical phenomena that may affect the measurement of scalar quantities by LIF are reported in the published literature. Our goal is to evaluate an experimental set-up for simultaneous measurements of velocity and concentration, using LDV and LIF. In a companying article in this proceedings (Lima et al, 2002), the two techniques are used to study the turbulent mixing between co-axial jets of large velocity ratio.

The organization of the paper is the following. Section 2 includes a brief analysis of the fluorescence signal. The experimental set-up and measuring equipment are described in Section 3, whereas Section 4 is concerned with the presentation and discussion of the results, including uncertainty analysis. The paper concludes with Section 5.

2. FLUORESCENCE SIGNAL CHARACTERISTICS

Fluorescence, a molecular process, is the return of an electron to the energy ground state by light emission, after absorption of light that caused the initial transition from the energy ground state to an excited state of energy. The frequencies of the emitted and absorbed lights are different (Stokes fluorescence). The fundamental equation to be used in LIF measurements is (Guilbault, 1990),

$$I_f = 2.3\phi I_0 \epsilon bc \quad (1)$$

where ϕ is the quantum efficiency, defined as the ratio between the emitted and the absorbed energy, I_0 is the incident light intensity, ϵ is the molar absorptivity and b is the absorption path length. Equation (1) is

valid for solutions with a low concentration of fluorescent dye, where the beam absorption along the path length is negligible, and expresses a linear response of fluorescent light intensity I_f to concentration c .

Nephelometry is a light intensity technique based on light dispersion (Mie scattering) principles of particles previously added to the flow, and the methodology proposed by Becker (1977) was extended to the LIF signal analysis. The fluorescence signal originated from the control volume is collected by the optical system and converted into the photo-multiplier output signal. Fluorescent light intensity detected by the optical system (I_r) is proportional to fluorescence emission (I_f), which depends on the volume averaged concentration of the fluorescent tracer in the measuring control volume (Becker et al., 1967)

$$\overline{I_r} = \Omega \int \overline{C} dV \quad (2)$$

with a fluctuation,

$$\overline{i_r^2} = \Omega^2 \overline{\left[\int c' dV \right]^2} \quad (3)$$

where Ω is the system optical efficiency, V is the control volume, and \overline{C} and c' are the mean and fluctuating concentration of the tracer in the control volume.

Fluorescence signal is converted by a photo-multiplier into an electrical output signal, and according with Becker et al. (1967) and Becker (1977) can be affected by 5 different types of noise: dark, incident light fluctuation, optical background, electronic shot and optical attenuation noise. The photo-multiplier mean response $\overline{I_A}$ is only affected by the background and dark noise, $\overline{I_b}$ and $\overline{I_d}$,

$$\overline{I_A} = \overline{I_r} + \overline{I_b} + \overline{I_d} \quad (4)$$

The optical attenuation noise is defined by the ratio between the actual fluorescence signal and signal in case there is no absorption along the optical path length. If the optical attenuation noise is negligible, the current mean quadratic fluctuation is,

$$\overline{i_A^2} = \left\{ \overline{i_r^2} + 2\overline{i_r i_b} + \overline{i_b^2} + \overline{i_0^2} + \overline{i_{esn}^2} \right\} \quad (5)$$

where $\overline{i_b^2}$ and $\overline{i_0^2}$ are the background radiation and the incident light fluctuations. The measured radiation fluctuation $\overline{i_r^2}$ is equal to the concentration turbulent fluctuation in the control volume $\overline{i_f^2}$.

The electronic shot noise fluctuation $\overline{i_{esn}^2}$ includes the background radiation and dark current fluctuations (Becker, 1977). The covariance ($\overline{i_r i_b}$) is difficult to measure or predict, and can be neglected, because

$$\left| \overline{i_r i_b} \right| < \sqrt{\left(\overline{i_r^2} \overline{i_b^2} \right)} \quad (6)$$

and i_r and i_b are of different wavelength and non-correlated, and $\overline{i_r i_b} \approx \pi \pi \overline{i_r^2} \overline{i_b^2}$. In our LIF signal analysis, the background radiation I_b noise and dark noise I_d were lumped into one single term designated zero-level (I_{zl}), corresponding to the light intensity measured by the photo-multiplier, without fluorescent tracer in the control volume. The mean zero-level was equal to,

$$\overline{I_{zl}} = \overline{I_b} + \overline{I_d} \quad (7)$$

and its mean quadratic fluctuation was defined by,

$$\overline{i_{zl}^2} = \left\{ \overline{i_b^2} + \overline{i_0^2} + \overline{i_{esn}^2} \right\} \quad (8)$$

In this way the mean measured fluorescence could be quantified by,

$$\overline{I_r} = \overline{I_A} - \overline{I_{zl}} \quad \text{and its fluctuation by, } \overline{i_r^2} = \overline{i_A^2} - \overline{i_{zl}^2} \quad (9 - 10)$$

3. EXPERIMENTAL SET-UP

3.1 Flow Configuration

Test Section. Measurements were carried out inside a Perspex tube 2 m long, 42 mm inner diameter and walls 4 mm thick. Optical access was made through an optical box, filled in with water to reduce refraction effects. Fluorescence measurements were made with the test section in a dark chamber to avoid the influence of ambient light and filled up with water of a known concentration of rhodamine B.

Simultaneous measurements of velocity and concentration were made in a coaxial jet geometry, consisting of a flow of known concentration of rhodamine B originating from an inner jet, 19 mm diameter, enclosed in the same Perspex tube.

Experimental Rig. The experimental rig (figure 1) was operated as an open circuit, with both the annular and inner jet circuits supplied by a centrifugal pump and controlled by a separate set of valves. Fluorescence measurements were made with the test section fed by the inner flow water circuit. Simultaneous velocity and concentration measurements were made using both inner and annular flows water circuits. The inner flow rate could reach values of $4.11 \times 10^{-4} \text{ m}^3 \text{ s}^{-1}$, measured by a rotameter with a resolution of 2% of its full scale ($8.22 \times 10^{-6} \text{ m}^3 \text{ s}^{-1}$). The annular jet flow rate was measured by a rotameter with a resolution of 1% of its full scale ($4.00 \times 10^{-5} \text{ m}^3 \text{ s}^{-1}$).

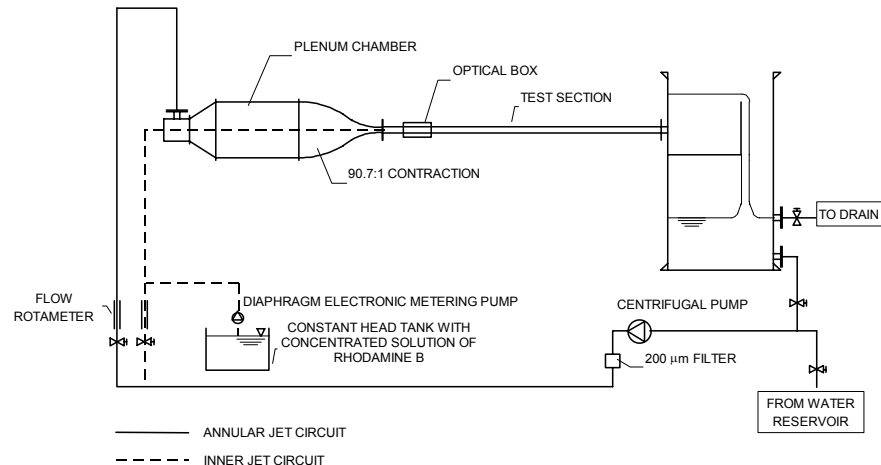


Fig. 1. Experimental rig

The annular jet flow was preceded by a converging nozzle with an area ratio of 90.7:1, at the extremity of a plenum chamber 600 mm long and 400 mm diameter. Inside the plenum chamber the flow went through 2 metal net screens, with an area of free area equal to 0.57 (Bradshaw, 1965), and 2 honeycombs, each with 30 mm length and 3.175 mm cells. This yielded an annular flow of uniform velocity profile and 6% axial turbulence intensity at the beginning of the test section. The inner flow, originated from a brass tube with a straight extension of 100 inner diameters length, i.e. 1700 mm, to ensure fully developed pipe flow at the inner jet outlet.

Injection Circuit. The flow with a uniform and known concentration of rhodamine B was achieved by injecting a known flow rate of base-solution in the inner flow. The main unit of the injection system was an electronic diaphragm-metering pump (Cole Parmer G74110-15), operating at a maximum stroke frequency (125 pulses per minute) and amplitude, which yielded a flow rate between 2.3 and 2.6 L/h, depending on the inner and annular flow rates. The rhodamine B base-solution, a highly concentrated solution, was kept in a constant head reservoir, with 30 L capacity, under uninterrupted stirring and isolated from the ambient light. The injection took place 196 tube diameters upstream of the test section, ensuring homogeneous concentration in the test section.

Fluorescent tracer: rhodamine B. The fluorescent characteristics of the rhodamine B do not change over a period of several hours when continually stirred in water (Arcoumanis et al., 1990; Saylor, 1995), as opposed to other fluorescent dyes. In addition, because of its low molecular diffusivity and a high Schmidt number, it is particularly suitable for studies of turbulent mixing.

3.2 Measurement Equipment

Optical system. The light source (figure 2 and table 1) was an argon-ion laser (Spectra-Physics, Stabilite 2017) operating in power stability mode at 514.5 nm. The maximum laser power used was 600 mW, because higher power damaged the surface of the optical box acrylic glass. The optical system was a conventional one-component laser Doppler Dantec 55× modular optics, with a 310 mm front lens.

Measurements were made with two optical configurations, A and B in Table 1, which differed in the length of the control volume, altered by changing the laser beams separation at the front lens, using the beam waist adjuster (Dantec 55×22) and a beam translator (Dantec 55×32). The cleanliness of the optical system, the meticulous alignment of the whole optical system and the location of the beam waist at the beam intersection were all very important to avoid the occurrence of optical aberration in the control volume, to increase the light intensity at the control volume and obtain a good signal to noise ratio.

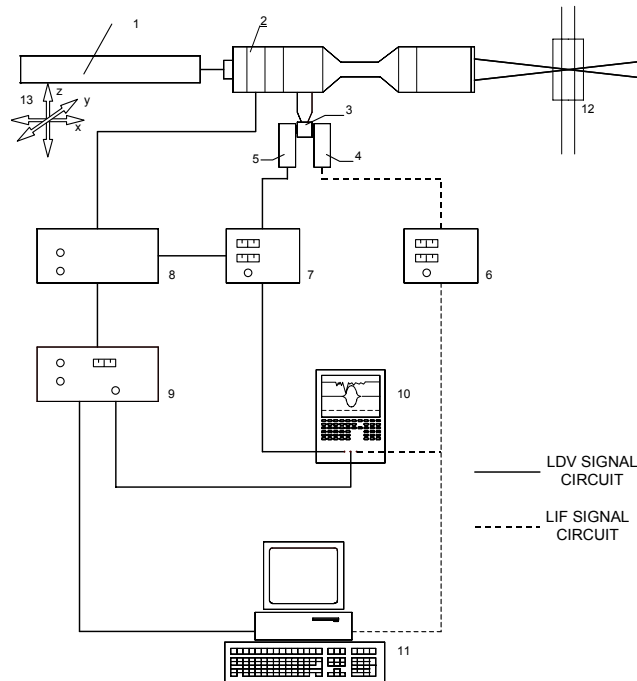


Fig. 2. Simultaneous LDV and LIF measuring equipment (1: Laser; 2: Optical system; 3: Colour separator with filters; 4: LIF photomultiplier; 5: LDV photomultiplier; 6: LIF PM power supply; 7: LDV PM power supply; 8: Frequency shifter; 9: Counter; 10: Oscilloscope, 11: Personal computer with velocimetry board and ADCM module; 12: Test section; 13: Optical bench mounted on a traversing table)

Both laser and optical system were mounted on a traversing table, with a resolution equal to 10 μm , along three perpendicular directions.

The collecting light system was common to both LDV and LIF optical signals, to guarantee that velocity and concentration signals originated from the same location. Although the fluorescence signal could originate from any location along the laser beams, the velocity signal could only be originated from the interior of the control volume after beam crossing. This would be particularly difficult in case of test section with curved walls.

The light collecting in backscatter was preferred to the forward scattering mode, though the latter is the preferred configuration in LDV measurements. Only the backscatter configuration ensured identical focusing conditions during the course of measurements; this was also possible because the fluorescent intensity had no preferential directions (Walker, 1987), contrary to the velocity Mie signal of the LDV system whose intensity is much reduced along the backscatter direction.

A colour separator split the collected light into 2 wavelengths, above and below 590 nm, which were filtered before reaching the corresponding photo-multipliers for velocity (514.5 nm interference filter, Dantec 55×37) and concentration (high pass filter, OG570 Melles Griot) signals. The photo-multipliers (Dantec 57×08) were fed by two separate power supplies. Particular care was taken in the design and assembling of the power supply for concentration signal, to avoid interference and reduce the electronic noise to values below the intensity of the concentration signal (Lima, 2000).

Table 1. Simultaneous LDV and LIF optical equipment characteristics

Argon-ion Laser (Spectra-Physics, model Stabilite 2017)	
Wavelength [nm] / Nominal output power [W]	514.5 / 1.8
Noise and stability in power mode operation [rms]	0.5 % / ± 0.5 %
Beam diameter at e^{-2} points [mm]	1.4
Optical system (Dantec, model 55× Modular Optics)	
Front lens focal length and aperture [mm]	310 / 79
Expansion of beams	$\times 1.94$
Pinhole section diameter [mm]	0.5
Configuration A	
Beam separation on front lens [mm]	39
Beam intersection angle in water	7.20°
Control volume dimensions in water (major and minor axis calculated) [mm \times mm]	1.584 \times 0.075
Fringe separation [μ m]	4.0970
Number of fringes without and with shift	18 / 73
Velocimetry conversion factor [MHz s m ⁻¹]	4.0970
Configuration B	
Beam separation on front lens [mm]	64
Beam intersection angle in water	4.43°
Control volume dimensions in water (major and minor axis calculated) [mm \times mm]	0.970 \times 0.075
Fringe separation [μ m]	2.5068
Number of fringes without and with shift	30 / 85
Velocimetry conversion factor [MHz s m ⁻¹]	2.5068

Data-processing. LDV data processing was made by a TSI Counter (1990C), operated at single measurement per burst mode (SM/B), for a 1% comparison between frequencies, estimated with 8 and 5 measurement cycles. Data acquisition of the concentration signal was performed using a 12-bit Analog Digital Converter Module of velocimetry board Zechs Electronics (1400A) installed in a personal computer (Dell 325 SX). Signals of velocity and concentration were acquired simultaneously, whenever the counter validated velocity.

4. RESULTS

To use LIF with confidence it is necessary to assess the response of the fluorescent tracer to experimental conditions, such as exposure to laser light, solution temperature, optical path length of the incident and collecting and other parameters whose importance will be addressed in this section.

4.1 Experimental Parameters

Changing of the fluorescence intensity with time.

Miller (1981) and Guilbault (1990), for instance refer that photo-decomposition of fluorescent tracer may occur. However, we found no such effect on measurements during 3 to 4 hours of continuously stirred solutions. The fluorescent signal was stable, regardless of the laser power, for homogeneous solutions with a concentration of 0.04 mg/L of rhodamine B.

Temperature

Measurements of fluorescence intensity were carried out for a range of temperatures between 25 and 40°C, of solutions of water and 0.04 mg/L of rhodamine B and a laser power of 200 mW. The results showed that a temperature increase of 1°C originated a decrease of approximately 2% in the fluorescence intensity, which was less than the 5% referred by Guilbault (1990). The dependence of rhodamine B on temperature has recently been used by Sakakibara and Adrian (1999) and Lemoine et al (1999) for simultaneous measurements of temperature and velocity; Sakakibara and Adrian (1999) report a decay of 2.3% K⁻¹, in line with our results.

Absorption

The absorption inside the test section (figure 3) can be quantified by τ_{mf} , the ratio between the signal at the opposite sides of path length ($x = 2$ and 21 mm). Values for low laser powers 200 mW do not show a

consistent trend and should be discarded. For laser powers of 400 mW and 600 mW one can see that the attenuation of light increases with both the concentration and laser power.

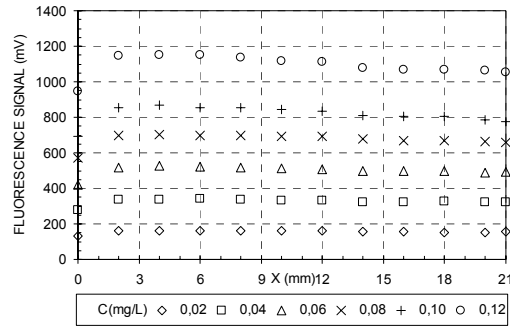


Fig. 3. Fluorescence intensity as a function of path length, for different concentration and 600 mW laser power

Table 3. Reduction of fluorescence intensity, τ_{mf} , between $x = 2$ and 21 mm as a function of laser power and rhodamine B concentration.

Concentration [mg/L]	Laser power		
	200 mW	400 mW	600 mW
0.02	100	89.9	94.3
0.04	93.9	88.6	94.5
0.06	90.3	91.8	93.4
0.08	99.0	92.0	93.4
0.10	96.0	88.6	89.7
0.12	91.1	89.9	90.3

Laser beams orientation and displacement

We measured radial profiles of mean concentration inside a horizontal flow with a homogeneous solution of rhodamine B, using concentrations of 0.042 and 0.064 mg/L. The laser beams were positioned in a horizontal plane and the control volume was moved along the horizontal and vertical diameters at the same tube section.

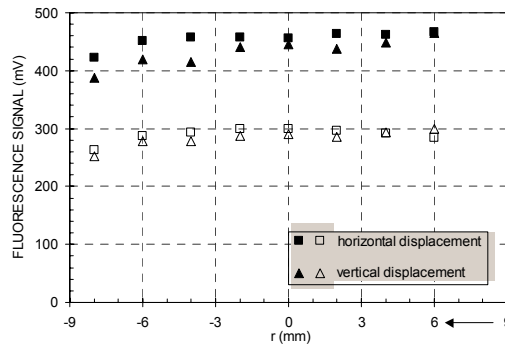


Fig. 4. Fluorescence intensity moving the control volume along the Perspex tube horizontal and vertical diameters, for 600 mW laser power and concentrations of rhodamine B equal to 0.042 mg/L (open symbols) and 0.064 mg/L (closed symbols).

The fluorescence intensity was always lower when moving the control volume along the vertical diameter, and this was more evident for increased optical path length and higher concentrations. When comparing measurements performed with the laser beams in a horizontal or vertical plane, i.e. configuration for axial and radial velocity measurements, (figure 5) lower fluorescence intensities were observed for the same concentration when the beams were in a vertical plane.

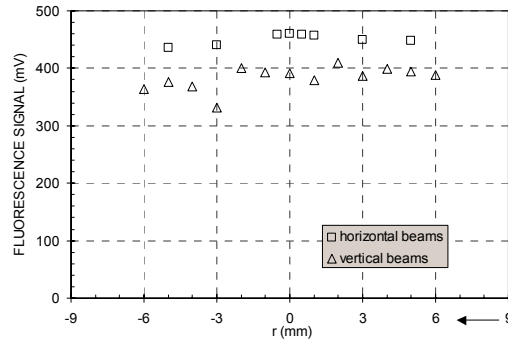


Fig. 5. Fluorescence intensity measured simultaneously with axial velocity (horizontal beams) and radial velocity (vertical beams) for 600 mW and a concentration of rhodamine B equal to 0.04 mg/L.

We concluded that in case of LIF measurements of flow inside a glass tube, the laser beams must be on the plane of longitudinal symmetry of the geometry.

Laser beams angle

The fluorescence intensity varies with the beam intersection angle and difficulties were expected when using LIF in geometries with curved surfaces. Figure 3 displays the intensity of the fluorescence signal as a function of the distance to a flat wall. The reduction of the angle between the laser beams (configurations A and B in Table 1) increased the length of the control volume and hence the light power and fluorescence signal intensity from 370 to 580 mV. Furthermore, because of the longer control volume, the interference of the test section walls changed from 2 mm away from the wall, in case of 8.86° to 6 mm for an angle equal to 5.42° . Configuration B, the larger angle had our preference, because of the lower influence of the wall.

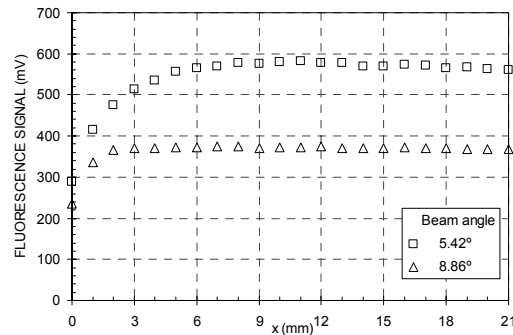


Fig. 6. Fluorescence intensity for optical configurations A and B (table 1), for a solution with 0.04 mg/L of rhodamine B and laser power equal to 400 mW.

Linear relationship between concentration and fluorescence intensity: calibration

Once the fluorescent tracer response to experimental conditions is known, the validity of equation (1) can be investigated. Figure 4 is the result of search for the linear relationship between concentration and fluorescent signal, for laser powers below 600 mW. The linear correlation gets worse as the laser power increases, but for concentrations under 0.08 mg/L there seems to be no influence of laser power. To show the repeatability, we include also experimental data associated with identical experiments performed in different days and using different batches of a highly concentrated solution of rhodamine B (open and closed symbols).

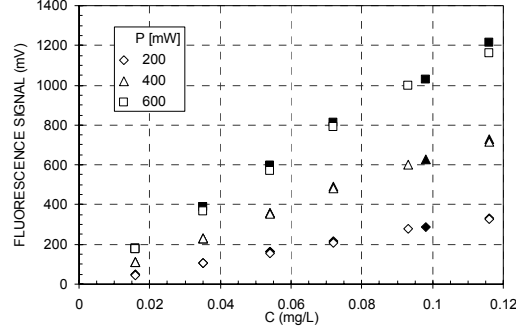


Fig. 7. Fluorescence intensity as a function of laser power and concentration (open and closed symbols correspond to identical experiments, performed in different days, to check the repeatability).

4.2 Uncertainty Analysis

Classical analysis. Experimental uncertainty analysis was based on the methodology by Taylor and Kuyatt (1994), as in the “Guide to the Expression of Uncertainty in Measurement” of the International Organization for Standardization (ISO). The combined standard uncertainty of the estimate r of the measurand R was defined by

$$U_R = \sqrt{U_A^2 + U_B^2} \quad (11)$$

where U_A and U_B are the standard uncertainties of type A and B, due to random and systematic effects. In case U_A and U_B are a combination of i independent quantities,

$$U_A = \sqrt{\left(\frac{\partial r}{\partial i} U_{Ai}\right)^2} ; U_B = \sqrt{\left(\frac{\partial r}{\partial i} U_{Bi}\right)^2} \quad (12)$$

The combined standard uncertainty in LIF concentration measurements (table 3) varied between 5.5 and 15.6 %, and is most influenced by the concentration parcel. Nevertheless for solutions with a concentration equal to 0.04 mg/L, which present a relative concentration uncertainty of 5.3 %, the relative combined standard-uncertainty varies between 7.6 and 5.6 %, for 200 and 600 mW laser powers.

The minimum combined standard-uncertainty was obtained from the combination between the minimum uncertainty of the emitted fluorescence signal (when concentration was low) and the maximum uncertainty of the processed fluorescence signal (when both concentration and laser power were low). Likewise the maximum combined standard-uncertainty was obtained combining the maximum uncertainty of the emitted fluorescence signal and the minimum uncertainty of the processed fluorescence signal.

Table 3. Relative uncertainties estimates for the measurement of concentration by LIF.

Parameter	Relative uncertainty [%]	
	minimum	maximum
Concentration	3.2	14.8
Laser Power	1.7	5.0
Emitted fluorescence signal	3.8	15.6
Processed fluorescence signal	0.2	4.0
Combined standard uncertainty	5.5	15.6

Statistical methods (bootstrap). Statistical analysis was also applied to the data, using a resampling procedure, the bootstrap (Efron and Tibshirani, 1993). The bootstrap is a computational statistical technique that provides confidence interval estimates for standard deviation, skewness and flatness without assumptions, such as normal distribution, which may not always be valid, when dealing with turbulence results. The technique is based on drawing from the data time series B random samples, where some elements may appear more than once. For each sample a replicate of the statistic being studied is calculated and the standard error is obtained calculating the standard deviation of the B replicates. It is observed that, for a high number of replications, the replicates distribution shows tendency towards a normal distribution, which allows the determination of an approximate 95 % confidence interval.

Though they are not very common yet in the analysis of turbulence experimental data, these techniques have gained increased popularity and are implemented in mathematical software packages. In case of Matlab, three lines are enough to build a confidence interval of the flatness (kurtosis) of a set of measurements, stored in a vector:

```
estimate=kurtosis(vector);
bootstat=bootstrp(200,'kurtosis',vector);
estimate_ci=1.96*std(bootstat);
```

Apart from established techniques for evaluating the experimental uncertainty, new, ad-hoc procedures can be devised depending on the flow characteristics, measurement techniques, etc.

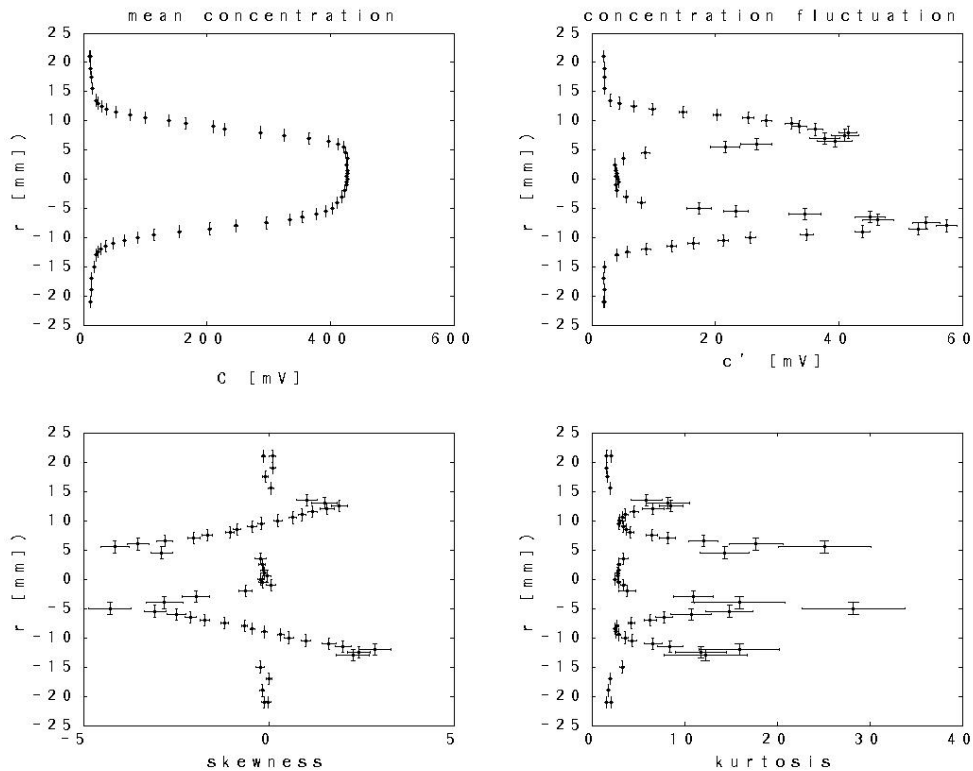


Fig.8. Uncertainty estimates based on the bootstrap technique. a) mean concentration; b) fluctuating concentration; c) skewness; d) flatness. The vertical error bars are the uncertainty due to position of the measuring control volume. Measurements at axial location $x/d_0 = 1$ and velocity ratio $U_d/U_{in} = 6.5$. For details refer to Lima and Palma (2002).

Mass conservation analysis. This is a confined flow and evaluation of mass and concentration flux, which should remain constant along the tube, is simple and can be used as an indicator of the general quality of the experimental data. The results of that exercise showed that the calculated mass flow rate was always below the value measured with a rotameter (on average, 96.3 %). The calculated concentration flux averaged, for the flow conditions presented here, was 73.8% of the injected flux. These differences are explained by the combination of uncertainties in the mass flow rates and concentration measurements.

Symmetry check. The geometry is axisymmetric and it is to be expected that all radial profiles be also symmetric. Deviations from symmetry may be caused by low quality or ageing of the Perspex tube, misalignment of the test section itself (during the assembling stage or later during the course of the measurements), misalignment of the laser traversing system with respect to the test section, etc. The profile symmetry is also a proof that the effects of attenuation are negligible, certainly lower than other

uncertainties involved. Otherwise, one would notice a decay in concentration with distance, and the results though located at identical distance from the tube centreline (radial distance) would be different.

5. CONCLUSIONS

1. In continuously stirred homogeneous solutions of low concentration the fluorescence intensity of rhodamine B remained constant with time. For concentrations up to 0.04 mg/L the light absorption along the beam path was less than 5% and did not affect the linear relationship between concentration and fluorescence intensity
2. The curvature of the cylindrical surface affects the intensity of the fluorescence signal. In case of measurements of flow inside a glass tube, the laser beams must be on the horizontal plane and concentration measurements made jointly with the axial component of velocity.
3. Despite of a lower fluorescence signal, a half-beam intersection angle equal to 5.89° was chosen, to enable measurements up to 2 mm from the wall.
4. The linear relationship between concentration of rhodamine B and fluorescence intensity was found for concentrations up to 0.08 mg/L and laser power below 600 mW.
5. The experimental uncertainty of concentration measurements was determined to be between 5 and 15%.
6. Based on the bootstrap technique, we could see that the confidence intervals downgraded as the order of the statistical moments increased. Flatness could be measured with a maximum uncertainty of about 25%

Acknowledgments

This experimental work was performed in the Hydraulics Laboratory of the Civil Engineering Department of the Faculty of Engineering of the University of Porto. The technical support of Mr. Jerónimo Sousa and the friendly interest of Dr. Fernanda Proença are gratefully acknowledged. The study is based in part on the doctoral thesis of the first author, under grants BD/2033/92/RN and BD/5623/95 of programmes *Ciência* and *Praxis XXI*, and was developed under research contract PEAM/C/APR/132/91, entitled *Dispersion Studies in Liquid Flows by Laser Induced Fluorescence*, and more recently also under project POCTI/33980, *BULET - Boundary Layer Effects and Turbulence in Complex Terrain*, all funded by the Portuguese Foundation for Science and Technology (FCT).

REFERENCES

- Arcoumanis, C., McGuiirk, J.J. and Palma, J.M.L.M. (1990). "On the use of fluorescent dyes for concentration measurements in water flows", *Experiments in Fluids*, **10**, pp. 177-180.
- Becker, H.A. (1977). "Mixing, concentration fluctuations, and marker nephelometry", in Launder, B.E., editor, *Studies in Convection*, volume **2**, pp. 45-139. Academic Press.
- Bradshaw, P. (1965). "The effect of wind-tunnel screens on nominally two-dimensional boundary layers", *Journal of Fluid Mechanics*, **22**, pp.679-687.
- Dantec (2000). "FlowMap Planar-LIF System. An overview of Dantec Dynamics's planar-LIF solutions for liquid applications. Dantec technical report. Available at http://www.dantecmt.com/Download/pdf_files/pi710112.pdf
- Efron, B. and Tibshirani, R.J (1993). "An introduction to the bootstrap". Chapman & Hall, USA.
- Guilbault, G.G. (1990). "Practical Fluorescence", 2nd edition. Marcel Dekker, Inc..
- Koochesfahani, M.M. (1984) "Experiments on Turbulent Mixing and chemical Reactions in a Liquid Shear Layer", PhD Thesis, California Institute of Technology, USA.

- Lemoine, F., Antoine, Y., Wolff, M. and Lebouche, M. (1999). "Simultaneous temperature and 2D velocity measurements in a turbulent heated jet using combined laser-induced fluorescence and LDA", *Experiments in Fluids*, **26**, pp. 315-323.
- Lima, M.M.C.L. and Palma, J.M.L.M. (2002). "Mixing in coaxial confined jets of large velocity ratio". In Proceedings of 11th International Symposium on Applications of Laser Techniques to Fluid Mechanics, 8-11 July, Lisbon, Portugal. Session 36, entitled *Mixing in Jets*.
- Lima, M.M.C.L. (2000). "Simultaneous Measurement of Velocity and Concentration by Laser Doppler Anemometry and Laser Induced Fluorescence" (in Portuguese), PhD Thesis, University of Porto, Portugal.
- Miller, J.N. (1981), editor. Standards in Fluorescence Spectroscopy. Ultraviolet Spectrometry Group, volume 2. Chapman and Hall.
- Nouadje, G., Siméon, N., Nertz, M. and Couderc, F. (1996). "Électrophorèse capillaire et detection par fluorescence induite par laser: différents montages de detection et leur application à l'analyse de très haute sensibilité d'amines et d'acides amines (revue)", *Analysis*, **24**, pp. 360-370.
- Owen, F.K.. (1976). "Simultaneous laser measurements of instantaneous velocity and concentration in turbulent mixing flows", AGARD N.193, Applications of Non-Intrusive Instrumentation in Fluid Flow Research.
- Saylor, J.R. (1995). "Photobleaching of disodium fluorescein in water", *Experiments in Fluids*, **18**, pp. 445-447.
- Sakakibara, J. and Adrian, R.J. (1999). "Whole field measurements of temperature in water using two-color laser induced fluorescence", *Experiments in Fluids*, **26**, pp. 7-15.
- Taylor, B.N. and Kuyatt, C.E. (1994). "Guidelines for evaluating and expressing the uncertainty of NIST measurement results", NIST Technical Note 1297, National Institute of Standards and Technology.
- Walker, D.A. (1987). "A fluorescence technique for measurements of concentration in mixing liquids", *Journal of Physics E: Scientific Instruments*, **20**, pp. 217-224.
- Wang, G.R. and Fiedler, H.E. (2000a). "On high spatial resolution scalar measurement with LIF. Part 1: photobleaching and thermal blooming", *Experiments in Fluids*, **29**, pp. 257-264.
- Wang, G.R. and Fiedler, H.E. (2000b). "On high spatial resolution scalar measurement with LIF. Part 2: the noise characteristic", *Experiments in Fluids*, **29**, pp. 265-274.
- Wild, G., André, J.-C., Grandclaudeon, M., Midoux, N. and Charpentier, J.-C. (1987). "Méthodes et instrumentation photophysiques pour le genie des procédés", *Entropie*, **137/138**, pp. 69-85.